NUMERICAL SIMULATIONS OF FLOW THROUGH AN S-DUCT

[1]Pravin Peddiraju, [1]Arthur Papadopoulos, [2]Vangelis Skaperdas, [3]Linda Hedges
[1]BETA CAE Systems USA, Inc., USA, [2]BETA CAE Systems SA, Greece, [3]CFD Consultant, USA

KEYWORDS – S-Duct, CFD, Propulsion, Aerodynamics

ABSTRACT –

Diffusing S-Ducts are critical components in certain military and civilian aircraft, primarily employed in directing airflow to the engine. Air flow through an S-Duct is complex in nature, and can include boundary layer separation, secondary flow, and total pressure loss effects that often impact engine performance. Thus, it is very important to accurately capture these effects in CFD simulations through a computational grid of appropriate resolution. This paper describes how ANSA, BETA CAE Systems' pre-processing software, was used to generate high fidelity grids for an S-Duct model that was featured at the 1st Propulsion Aerodynamics Workshop (PAW). This paper also presents numerical simulation results of flow through the S-Duct. Metacomp Technologies' CFD solver, CFD++, was used for numerical simulations and BETA CAE Systems' software, µETA, was used for post-processing.

KEYWORDS –
Validation, S-DUCT, PAW, Propulsion Aerodynamics Workshop, Grid Generation

1. INTRODUCTION

Diffusing S-Ducts are critical components of military and civilian aircraft, primarily employed to direct airflow to the engine. Airflow through an S-Duct is fundamentally complex in nature. While not desirable, it often involves boundary-layer separation and total-pressure loss effects that impact engine performance. These losses and the secondary flows introduced by the serpentine shape create a complex flow field that is challenging to predict numerically.

Accurately capturing these effects in CFD simulations requires a computational grid of sufficient resolution without excess grid. Superfluous grid adds cost by driving up computing resource requirements and slowing turn-around time. As a result, fewer design permutations can be investigated, impeding the ability to explore a comprehensive design space.

This paper describes how ANSA, BETA CAE Systems' pre-processing software, was used to generate high fidelity grids for an S-Duct model and also presents numerical simulation results of flow through the S-Duct. The Metacomp Technologies' CFD solver, CFD++, was used for numerical simulations and BETA CAE Systems' software, µETA, was used for post-processing.

Section 2 discusses the experimental and computational set up for the S-Duct validation case. Section 3 presents the CFD case selection, where a variety of grid comparison choices are made. Comparisons include matching equivalently-resolved structured- and unstructured-grids, full versus symmetric domains, and structured and unstructured grid resolution studies. Section 4 compares CFD results to experimental data. Section 5 presents the results of grid comparisons. Section 6 demonstrates grid generation for the S-Duct with flow-control devices. Finally, conclusions are presented in Section 7.

As a side note, the S-Duct model described here was featured at the 1st and 2nd Propulsion Aerodynamics Workshops (PAWs). The Propulsion Aerodynamics Workshop is sponsored by the AIAA Air Breathing Propulsion Systems Integration Technical Committee (reference). The stated objectives of the workshop are to: (1) Assess the predictive capability of selected

CFD methods when applied to aerodynamic flows associated with air breathing propulsion, and (2) Develop process guidelines for the numerical simulation of inlet, nozzle, and jet flow fields.[1,2] The workshops provide collaborative opportunities to run validation cases with colleagues from around the world, and enable comprehensive investigations regarding many aspects of numerical solutions, including flow solvers, turbulence models, grid types, and grid resolution.

2. EXPERIMENTAL AND COMPUTATIONAL SETUP

Experimental Model

The validation case selected by the workshop committee is the ONERA Serpentine diffuser S-duct configuration shown in Figure 1[3]. The model includes a bellmouth, a constant diameter pipe, and an S-shaped duct. The bell mouth entrance of the S-Duct is representative of inlet flow.
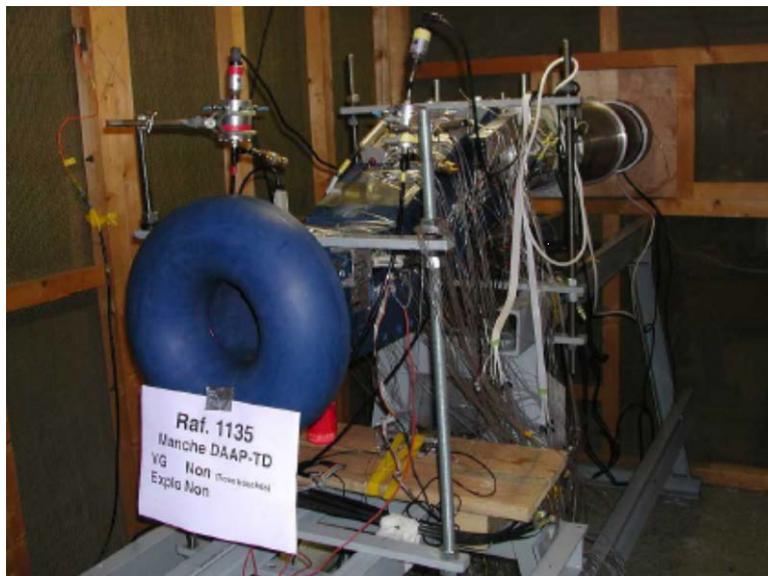

Figure 1: ONERA S-Duct Test Apparatus

The goal of the test was to generate experimental data both with and without flow control devices as a means to validate the different turbulence models used with Navier-Stokes calculations. The experimental setup drew air in from the surrounding atmosphere. Mass flow was controlled at the diffuser end. The inflow pipe diameter is 0.133 meters. The Reynolds number is about 1.5 million with an entrance Mach number of approximately 0.6.

Three rows of static pressure measurements were taken along the duct surface. A 40 Kulite rake was placed at the Aerodynamic Inlet Plane (AIP). Hot wire measurements provided the boundary layer thickness just upstream of the flow separation. Various flow control device setups were tested including a configuration with eight vortex generators. The vortex generator vanes were located in a single row at the start of the serpentine dip.

Static pressure measurements, pressure recovery, pressure distortion, and upstream boundary layer profiles were made available for comparison to CFD data. The first PAW workshop was a "blind" comparison, and data was made available for the second PAW workshop.

Flow Solver

The CFD results presented here were calculated with the flow solver CFD++. CFD++ is a powerful commercial software suite developed by Metacomp Technologies, Inc[4]. It combines

the accuracy of research codes with the robustness and versatility of a commercial solver. CFD++ allows for the treatment of complex geometries with a variety of mesh possibilities including structured, unstructured, multi-block, and overset grids, including overset unstructured grids.

A total-variation diminishing algorithm with a powerful algebraic multi-grid solver is used. The preconditioner was used for cases with free-stream Mach number less than 0.3. CFD cases were run at low cost on the Amazon Cloud with 32 to 128 cores and a 10G Ethernet connection.

Flow solutions were evaluated using residual and mass-flow convergence, reliably obtaining over 4 orders of residual convergence and target mass-flow convergence to less than 0.1%.

The CFD cases presented here used both "structured" and hybrid unstructured (prism, tetrahedral, pyramid) elements.

CFD Geometry, Grid and Boundary Conditions

The CFD domain is shown in Figure 2. The far-field boundary condition is 10 diameters upstream to simulate a plenum. The upstream boundary condition, shown in green, is a reservoir boundary condition that holds total pressure and total temperature at input values. The duct outflow boundary condition is an iterative mass-flow boundary condition. Pressure is adjusted to match the requested mass flow. The duct outflow boundary condition is shown in yellow. The symmetry boundary condition is shown in pink. A solve-to-the-wall boundary condition was used on the pipe, plug, and vortex generator geometry. The vortex generator configuration is shown in Figure 3.
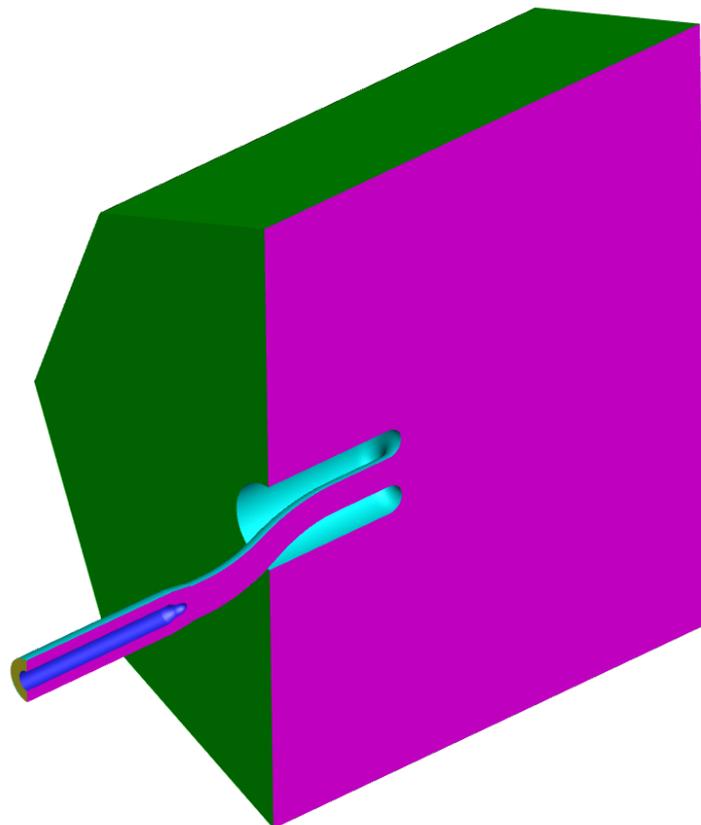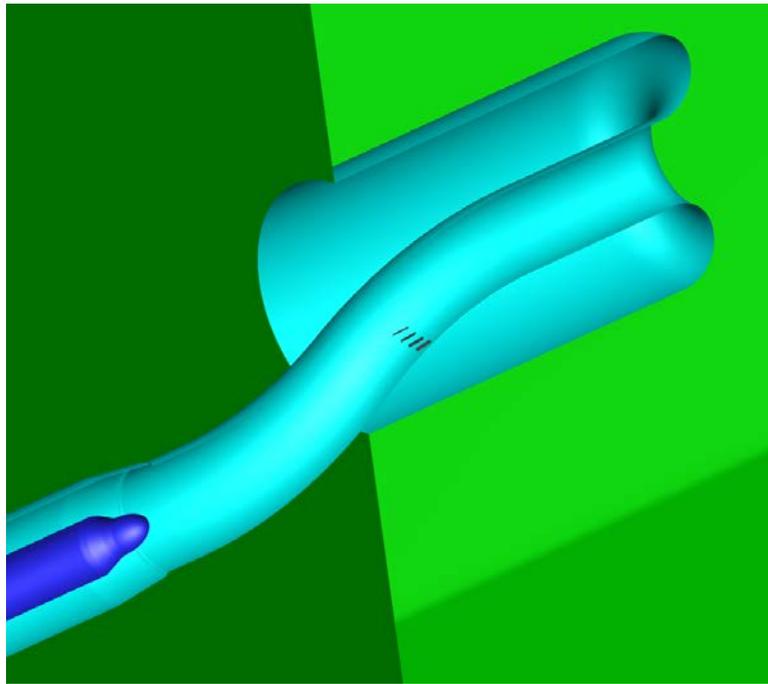

Figure 2: Computational domain

Figure 3: Vortex Generator Configuration

3. CFD COMPARISON CASES AND GRID GENERATION

A variety of S-Duct comparisons were made including:

- Equivalently resolved structured and unstructured grids
- Grid resolution investigations
- Full vs symmetry models
- SST vs Cubic k-ε turbulence models
- With and without vortex generators

All grids were generated using Beta CAE ANSA[5].The list of the comparison S-Duct grids is shown in Table 1.

Table 1: S-Duct Grids Generated

Name	Size	Model	Grid Count	Layer Growth Rate	Y+
Unstructured	Fine	Full	31.2 M	1.2	0.9
Unstructured	Med	Full	12.6 M	1.2	0.9
Structured	Fine	Full	10.7 M	1.2	0.4
Structured	Med	Full	4.2 M	1.2	0.4
Structured	Med	Half	2.1 M	1.2	0.4
Structured-VG	Fine	Half	16M	1.2	0.4
Unstructured-VG	Fine	Half	37M	1.2	0.4

While grids were provided to workshop participants, the goal of this effort was to develop better grid-generation techniques and the PAW-committee-provided meshes were not used.

Unstructured meshes were generated with the batch mesher in an automated framework. Structured meshes were generated with the hexa-block mesher. Grid spacing was based on curvature-based seeding.

An example unstructured grid is shown in Figure 4 and an example structured grid is shown in Figure 5. Please note that while the ordered mesh is called "structured", all meshes were run with CFD++, an unstructured flow solver.
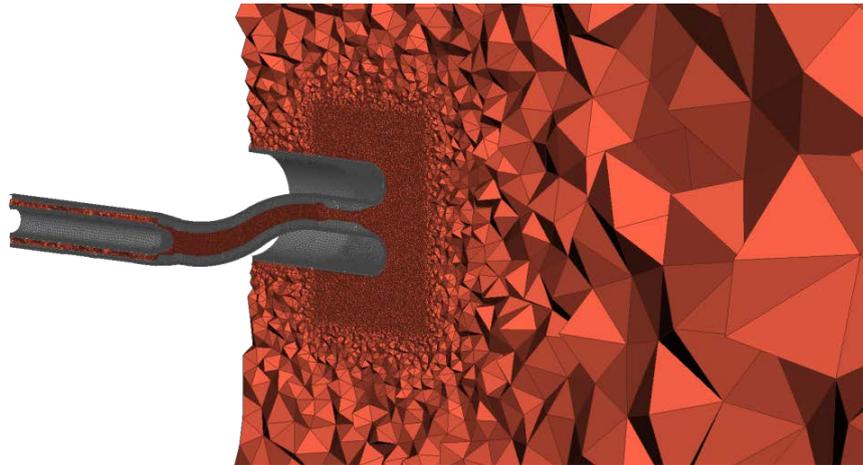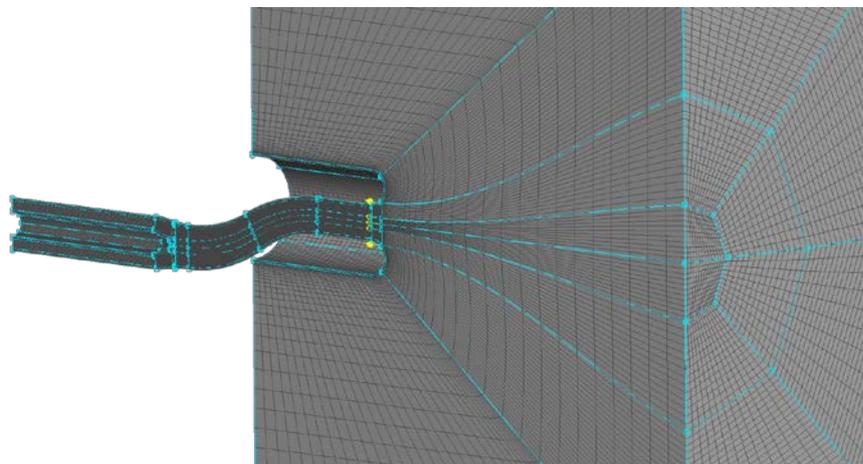

Figure 4: Medium Unstructured Grid

Figure 5: Medium Structured Grid

4. COMPARISON TO EXPERIMENT

The authors of this paper focused on S-Duct grid-generation as their contribution to the first PAW workshop. However, PAW 1 was a blind comparison to experimental data. The experimental validation data for the S-Duct CFD cases were not released until after PAW 1, allowing participants to evaluate their techniques in a "blind" comparison to the experimental results. Following PAW 1, the committee released a paper discussing all of the CFD results submitted by all participants and comparing those results to experimental data. These results are found in Reference 6.

As the S-Duct data is now available to participants, this paper offers a quick comparison of our CFD results to the Reference 6 figures in Figures 6 and 7 of this paper. The CFD data is

given on the left-hand-side and the experimental data is on the right-hand-side. For more information on the comparison of all CFD results to experimental data, please see the referenced paper.
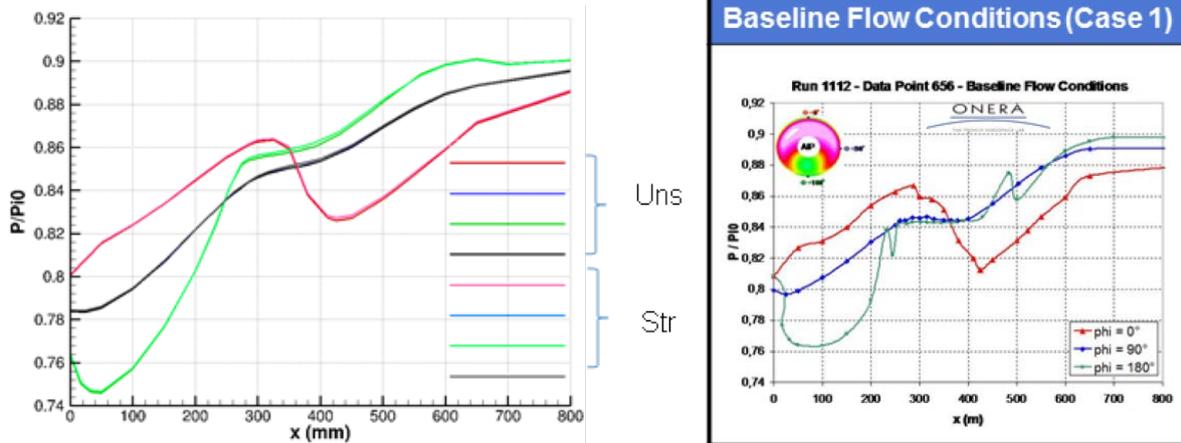

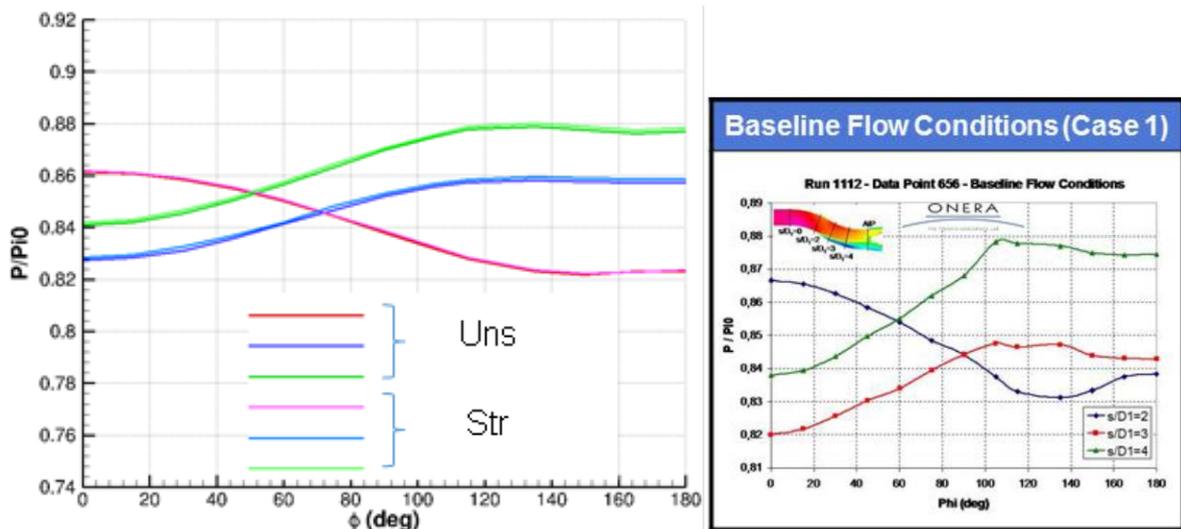**Figure 6: Experimental Comparison of Pressure (Reference 6)**

Figure 7: Experimental Comparison of Pressure (Reference 6)

To generalize the conclusions from Reference 6, most participant results were relatively close to each other and approximately to the experimental data, but none of the CFD solutions matched the experimental data precisely.

Experimentally determined boundary layer profiles are shown in Figure 8. Workshop participants were asked to run with fully developed turbulent boundary layer profiles. Computationally predicted boundary layer profiles were thus fully developed and symmetric.

As seen in Figure 8, the measured entrance profiles do not appear to be fully developed or symmetric. Perhaps the Reynolds number is low enough to require a model of transition to capture these profiles and the subsequent separation with precision. Otherwise, the cause of the relatively small but persistent deviation between the analysis and experimental results is unclear.
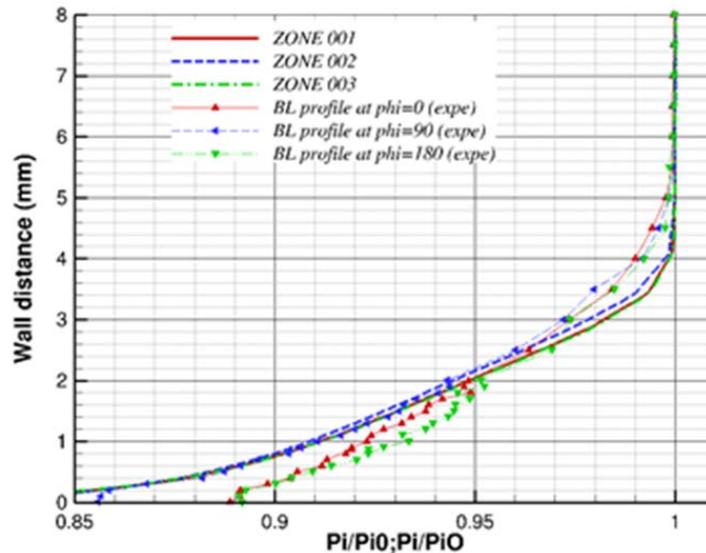
Figure 8: Experimentally Measured Boundary Layer Profiles (Reference 6)

5. RESULTS OF CASE COMPARISON

Many grid and analysis comparisons were made to understand the modelling of the S-Duct flow and pipe flow in general. Table 2 lists the CFD cases run. Included in the table is the final mass flow obtained. Since the mass flow boundary condition was solved iteratively, a comparison of the final mass flow to the value targeted offers a measure of case convergence.

Table 2 also lists the final back pressure value from the CFD solution. The final back pressure is an indication of the total loss through the pipe. It is a first-order measure of the degree of similarity between cases for the fixed mass flow.

Except as noted, all flow solutions were run with the SST turbulence model.

Table 2: List of CFD Cases Run

NAME	TYPE	MASS FLOW (KG/S)	BACK PRESS (PA)	MODEL	TURB. MODEL
UNSFINESST	UNS	2.427	79855.6	FULL	SST
UNSMEDSST	UNS	2.428	79065.4	FULL	SST
UNSMEDCKE	UNS	2.426	79762.5	FULL	CUBIC K-ε
STRFINESST	STR	2.427	79881.0	FULL	SST
STRMEDSST	STR	2.427	79866.0	FULL	SST
STRMEDHALF	STR	1.214	79864.2	HALF	SST

Full Pipe Model Compared to a Symmetric Model

The application of a symmetric boundary condition allows for the modelling of only one-half of the complete S-Duct. Its use offers the potential of conserving the total computer-time required for a CFD case. Unfortunately, fluid flow is often asymmetric, particularly when flow-field separation is present. The symmetry plane in the S-Duct configuration cuts through the center of a separated region and this puts the application of a symmetry BC into question for this configuration. The instructions from the PAW committee were to run the S-Duct calculations with a symmetry condition. To ensure that this assumption of symmetry was appropriate for the steady-state flow calculation, a comparison was made between the full- and half-model simulation. The comparison of total pressure recovery is shown in Figure 9 at the downstream AIP (Aerodynamic Interface Plane).
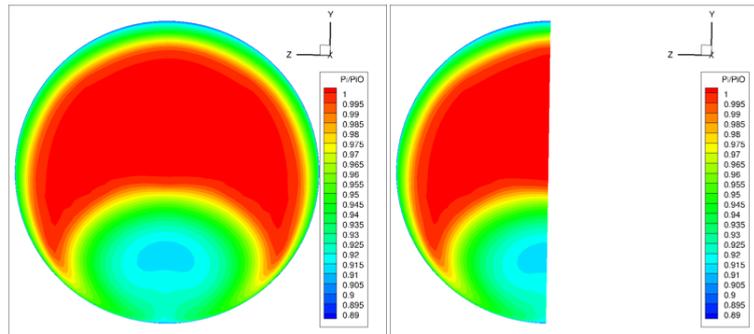

Figure 9: Comparison of Full versus Symmetric S-Duct Model

The comparison was based on the medium grid resolution structured mesh. Mass flow between the two cases matched to within 0.05% (half the total mass flow was used for the half-model case). The downstream static pressure value combined with the total pressure recovery contours demonstrate an excellent comparison and the validity of the symmetry boundary condition for this case.

Nonetheless, as resources were not considered to be an issue, the full model was used for subsequent S-duct cases in keeping with best practices for analyzing a flow field that may include separation.

Grid Resolution Investigations

Medium and fine grid resolutions are presented here and compared to each other for both unstructured and structured grids.

Figure 10 and 11 compare four cases:

1. Medium unstructured grid in the upper left
2. Medium structured grid in the upper right
3. Fine unstructured grid in the lower left
4. Fine structured grid in the lower right

Figure 10 shows Mach contours through the duct and Figure 11 shows total pressure recovery contours at the AIP.

Little difference is seen between the structured medium and structured fine grid flow solutions. The grid size is approximately doubled between the two grids (a multiple of root 2 in all directions). The AIP back-pressure variation between the two cases is less than 0.05% emphasizing their similarity. The medium structured mesh is adequate for a high quality flow solution.
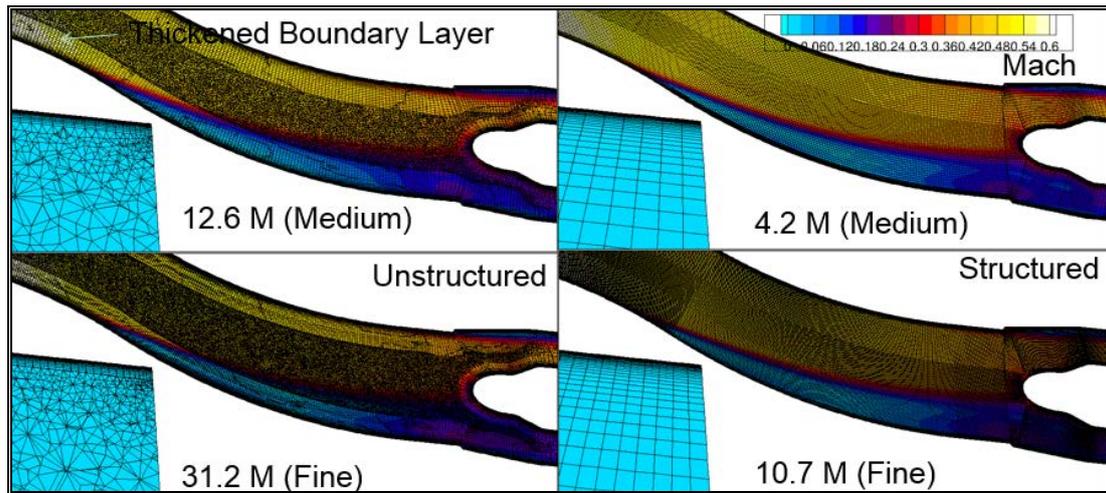
Figure 10: Grid Resolution and Type Comparison, Mach through the Duct

A notable difference is seen between the unstructured medium and unstructured fine grid flow solutions. The back pressure variation between the medium and fine grid unstructured mesh is about ~1%. The fine unstructured mesh downstream pressure matches that of the fine structured mesh showing that the fine unstructured mesh is required to achieve an adequate flow solution.
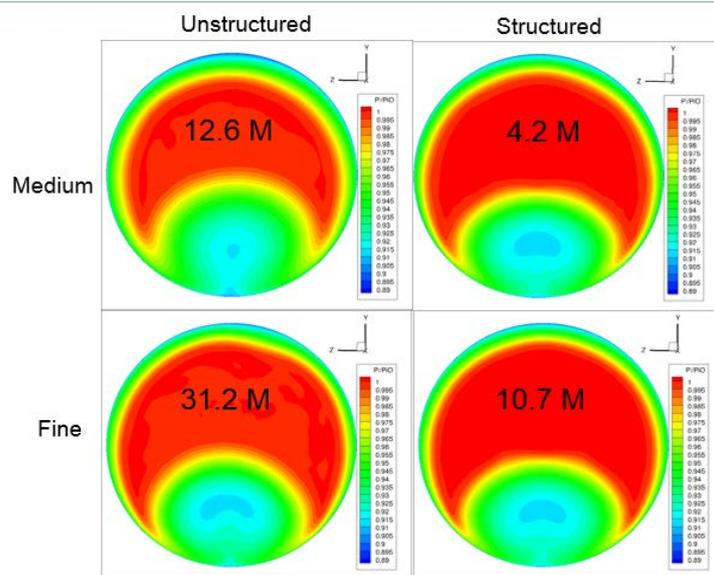

Figure 11: Grid Resolution and Type, Total Pressure Recovery at the AIP

Equivalently Resolved Unstructured and Structured Grids

A significant difference in flow solution is seen between the structured medium and unstructured medium grid flow solutions. An attempt was made to keep fundamental cell size of the grid the same between these two mesh setups. The isotropic nature of the tetrahedra with the unstructured mesh means that more mesh is required to achieve a roughly equivalently sized grid cell. Thus, the medium structured mesh outperforms the unstructured medium mesh despite the unstructured medium mesh containing far more total mesh cells

than the structured medium mesh. The medium structured grid mesh was able to achieve a more greatly resolved flow solution with about 4.2 million mesh cells. The unstructured grid required about 31.2 million mesh cells to achieve a similarly resolved flow solution.

These results suggest that approximately an order of magnitude more unstructured mesh is required to match an equivalent structured grid in terms of accuracy, at least in the presences of significant shear flow as seen with the S-Duct.

The Comparison of the SST Turbulence Model to the Cubic k-ε Turbulence Model

Two turbulence models were compared to each other for the S-Duct using the medium unstructured grid. For this comparison, the SST turbulence model was compared to the non-linear "cubic" k-ε model[4]. The SST model was used for all other CFD calculations presented in this paper.

The SST model is a two-equation model. It solves the transport equations for the turbulence kinetic energy (k), and for the turbulence inverse time-scale (ω). The latter is modified such that its dissipation blends from that of a k-ω formulation in the near-wall regions to that of a k-ε formulation away from walls and in wake regions.

The second analysis used the non-linear "cubic" k-ε model. The cubic k-ε model solves transport equations for the turbulence kinetic energy (k) and its dissipation rate (ε). While the model is also a two-equation model, this model has non-linear terms which account for normal-stress anisotropy, swirl, and streamline curvature effects.

Both turbulence models allowed for steady state and were well converged. For the most part, the two turbulence models predicted very similar flow solutions. On the medium level unstructured grid, the SST model had a thickened boundary layer and a slightly bigger separated region when compared to the cubic k-ε model. Figure 12 shows the thicker boundary layer and the slightly greater resulting separation.
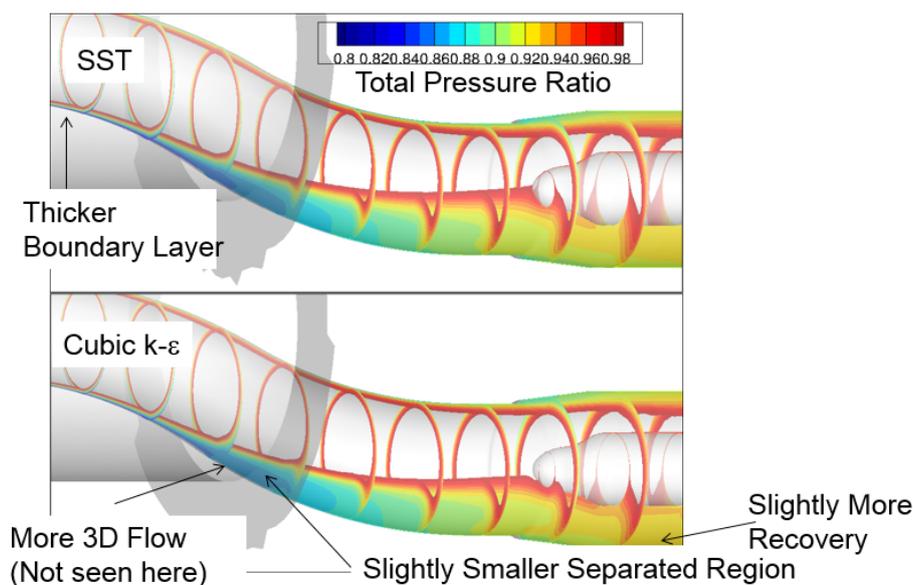

Figure 12: Turbulence Model Comparison on the Unstructured Medium Mesh

As shown in Table 2, the back pressure for the S-Duct analysis run with the SST model was approximately 1% lower than the back pressure for CFD case run with the cubic k-ε model.

Combined with the thickened boundary layers, this suggests that the SST model may be more dissipative. The cubic k-e model compared more favorably to the higher grid density SST solutions. However, a solution with the high density grid and the cubic k-ε turbulence model was not run and this would be necessary to know more about the dissipative effects of the turbulence models on lower resolution grids.

6. DUCT WITH FLOW CONTROL

The geometry for modelling the S-Duct with vortex-generator flow-control devices was provided during the PAW 2 workshop. Experimental results for this configuration are also given in Reference 3. Two grids were created to model the flow control devices in the S-Duct. Figure 13 shows the structured and unstructured grids generated for the vortex generator simulation. Eight counter-rotating vortex generators are aligned in a row as shown in Figure 14. Both grids are very high quality though it's clear that the structured mesh requires far fewer total cells. Both meshes were made quickly with the ANSA software. As the results from Section 5 indicate, it is likely that the structured grid requires fewer computational resources and also that the flow solution is of higher quality than a higher density unstructured mesh. A flow solution using CFD++ was only performed on the structured grid.
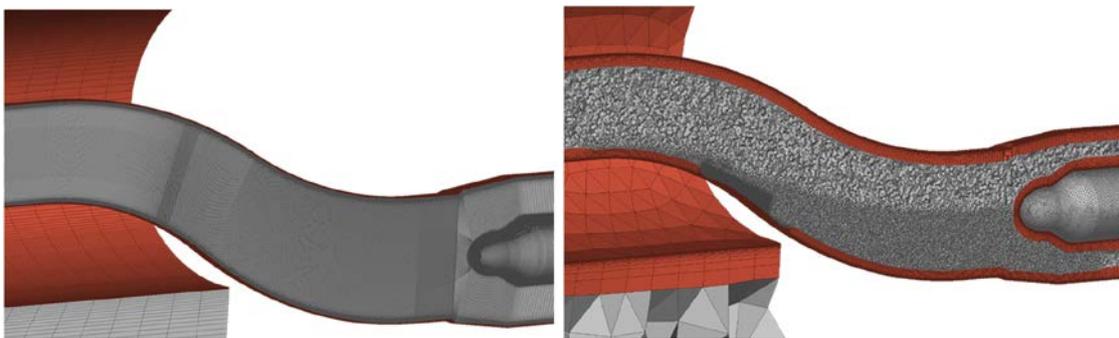

Figure 13: Structured (left) and unstructured (right) mesh for the S-Duct with VG's
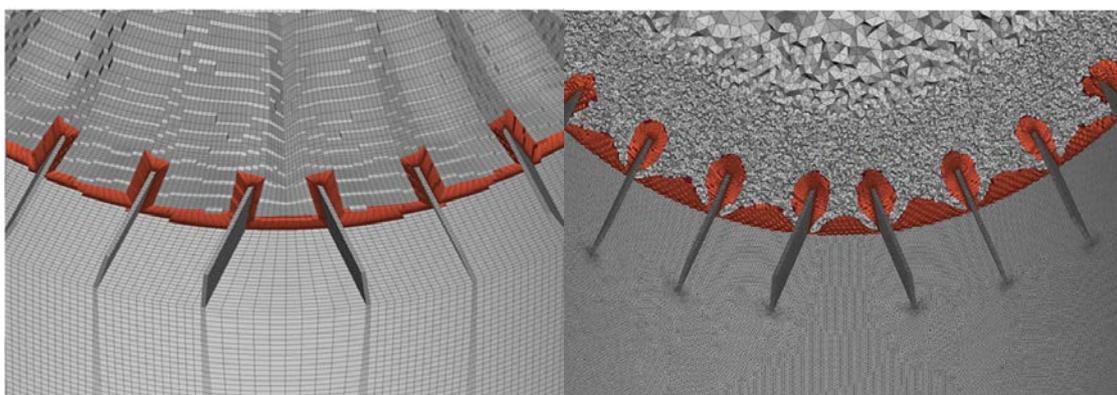

Figure 14: Structured (left) and unstructured (right) mesh for the S-Duct with VG's

Mach contours shown in Figure 15 demonstrate that the S-Duct separation as seen in Figure 10 is successfully eliminated by the VG's. This demonstrates the ability of the mesh to adequately resolve the vortex generated by the VG's and resolve its effect on the downstream flow field.
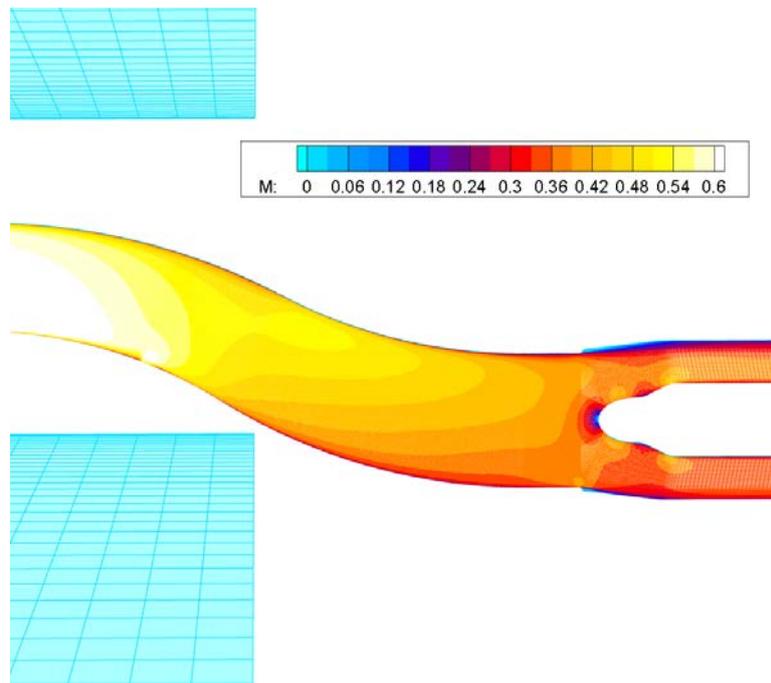
Figure 15: Flow solution for the S-Duct with VG's modelled with a structured grid

Total Pressure contours in the vicinity of the vortex generators in the S-Duct show the fine details of the flow field. The vortices generated by the vortex generators are clear as is their interactions such as downstream pairing.
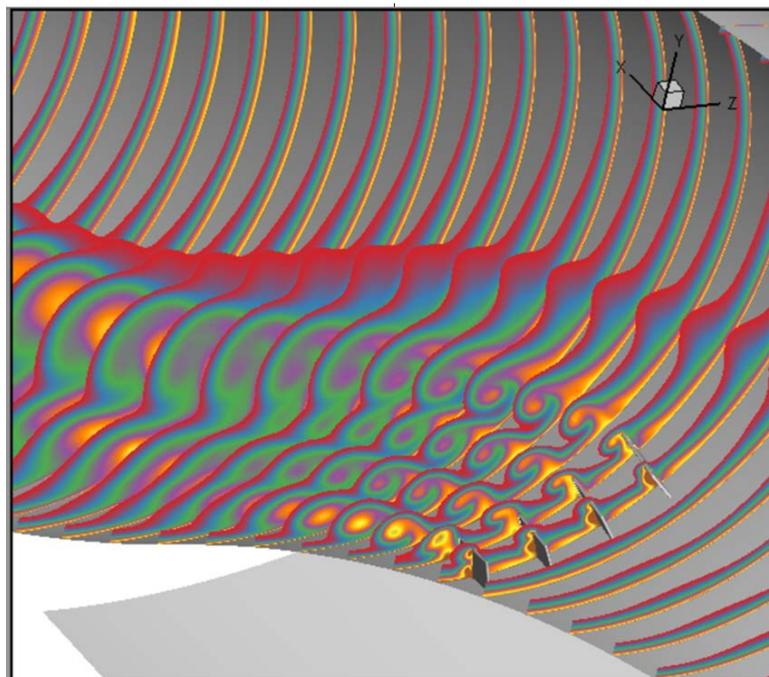

**Figure 16: Total pressure contours in the S-Duct near the VG's**

7. CONCLUSIONS

Navier-Stokes tools are essential for the analysis of engine inlet and nozzle designs. The optimization of air-breathing engine inlets requires maximizing inlet pressure recovery while minimizing fan-face distortion. Tools used in the design of these components must be well understood and reliable. The validation of solver methods against experimental data

becomes a critical step in the development and understanding of these tools as they are applied to the design of these components. Of particular interest is the opportunity to validate and demonstrate grid-generation methods. This paper discussed a variety of grid comparisons in the hopes of providing more insight into grid generation methods.

In summary:

- Structured and unstructured grid generation on complicated S-Duct geometries was reliable, efficient, and quick.
- The HexaBlock tool in ANSA produced reliable "structured" meshes which achieved superior performance to a regular hybrid unstructured mesh. Nonetheless, the unstructured meshes generated were of high quality.
- For the S-Duct case modelled, grid convergence was achieved and turbulence model differences were very small.
- A symmetry plane was acceptable and is likely acceptable for many cases that achieve convergence.
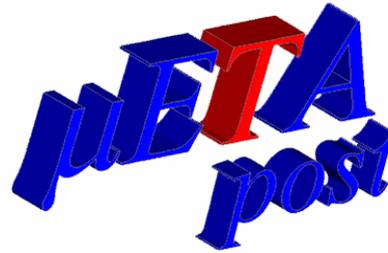
REFERENCES

(1) http://aiaapaw.tecplot.com/2012_Workshop/
(2) http://www.aiaa-propulsionenergy.org/PAW02/
(3) Delot, A, Garnier, E., "Flow Control in a High-Offset Subsonic Air Intake", AIAA 2011-5569.
(4) http://www.metacomptech.com
(5) ANSA version 12.1.5 User's Guide, BETA CAE Systems S.A., July 2008.
(6) Delot, A., Scharnhorst, R. K., "A Comparison of Several CFD Codes with Experimental Data in a Diffusing S-Duct", AIAA 2013-3796.

(7) μETA PostProcessor version 6.2.0. User's Guide, BETA CAE Systems S.A., June 2008